Anomalous nucleation events during crystallization of zeolite A under marginal alkalinities: A population balance analysis

Sanja Bosnar, Josip Bronić, Tatjana Antonić Jelić and Boris Subotić*

Ruđer Bošković Institute, Division of Materials Chemistry, [1]Laboratory for the Synthesis of New Materials and [2]Laboratory for the Precipitation Processes, Bijenička 54, 10000 Zagreb, Croatia

Supplementary Information

SI-1: comparison of the growth kinetics of zeolite A crystals having different morphologies

In order to better comparison the growth kinetics of zeolite A crystals having different morphologies, from the one side, and because the particle (crystal) size in the measured crystal size distribution curves are expressed as the equivalent spherical diameter, D (see Fig. 2 in the paper) from the other side, all the values of L (the distance between two opposite {001} crystal planes) are recalculated to the corresponding equivalent spherical diameter i.e.,[48]

$$D_\mathrm{m} = (1/F_1)\times L_\mathrm{m} \tag{SI-1.1}$$

where D_m and L_m are the corresponding sizes (dimensions) of the largest crystals and F_1 (see Table SI-1.1) is the shape factor. Fig. SI-1.1 shows the simultaneous changes of L_m (measured from optical microscopy images) and D_m (calculated by Eq. (SI-1-1), using the corresponding values of L_m, during crystallization of zeolite A in sub-systems S1-1, S1-6, S2-1 and S2-3 (see paper), as examples.

Table SI-1.1 Numerical values of the factor F_1 used for calculation of equivalent spherical diameter of different morphological forms of zeolite A in all used systems.

System	F_1
S1-1/S2-1	0.806/0.853
S12	0.824
S1-3/S2-3	0.840/0.853
S1-4/S2-4	0.903
S1-5/S2-5	0.903/1.000
S1-6	0.903
S1-7/S2-7	0.903/1.000
S1-8	0.903

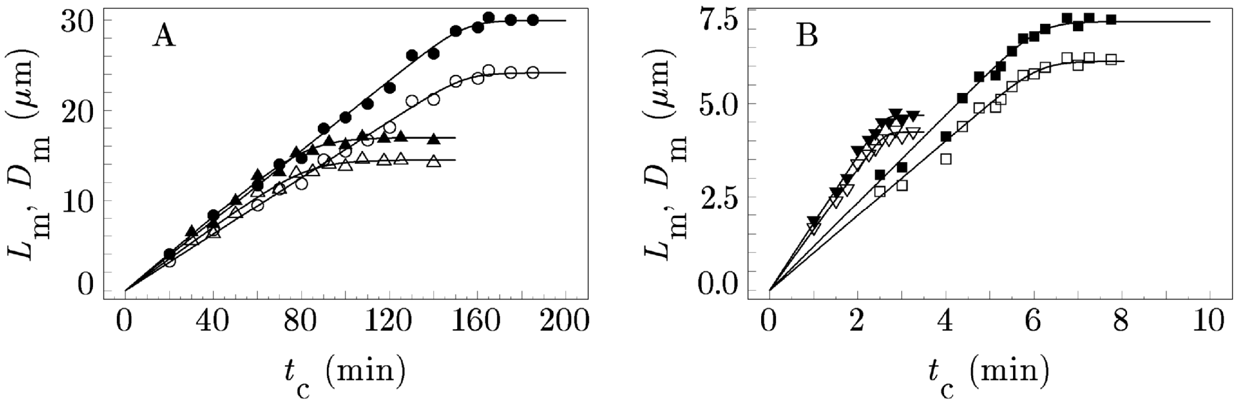

Fig. SI-1.1 Changes of the sizes L_m (○,△,▽,□) and D_m (●,▲,▼,■) of the largest zeolite A crystals during crystallization in systems S1-1 (○,●), S2-1 (△,▲), S1-6 (▽,▼) and S2-3 (□,■).

SI-2. Population balance of the crystallization processes and the principles of simulation

The population balance for zeolite crystallization in a well mixed, isothermal, constant volume batch crystallizer, i.e., under the conditions characteristic of most zeolite syntheses, may be defined by a set of ordinary differential equations,[3,4,7,36-40,68,69] i.e.,

$$\mathrm{d}m_o/\mathrm{d}t_c = \mathrm{d}N/\mathrm{d}t_c \qquad \text{(SI-2.1)}$$

$$\mathrm{d}m_1/\mathrm{d}t_c = Q\times m_o \qquad \text{(SI-2.2)}$$

$$\mathrm{d}m_2/\mathrm{d}t_c = 2\times Q\times m_1 \qquad \text{(SI-2.3)}$$

$$\mathrm{d}m_3/\mathrm{d}t_c = 3\times Q\times m_2 \qquad \text{(SI-2.4)}$$

where $m_i = \int D^i\times(\mathrm{d}N/\mathrm{d}D)\mathrm{d}D$ is i-th (i = 0, 1, 2, and 3) moment of the particle size distribution of zeolite crystals at crystallization time t_c, $\mathrm{d}N/\mathrm{d}t_c = B$ is the rate of nucleation, dN is differential number of nuclei released from the gel matrix in the differential crystallization time dt_c, $Q = \mathrm{d}D/\mathrm{d}t_c$ is the rate of crystal growth and dD is differential change in the crystal size (e.g., equivalent spherical diameter, D) in the differential crystallization time dt_c.

Many analyzes of the relationship between $f_N = N/N_0$ and $f_c = m_c/m_c(\mathrm{eq}) \approx f_G^* = m_G^*/m_G^*(0)$ (N is the number of nuclei "released" from the mass, m_G^*, of gel needed for crystallization of the mass, m_c, of zeolite, N_0 is total number of nuclei in the gel matrix, $m_G^*(0)$ is the entire amount of the dissolved gel and m_c(eq) is the mass of crystallized zeolite at the end of crystallization process, $t_c = t_c(\mathrm{eq})$) showed that the relationship may generally be expressed by three-parameter equation,[3,4,7,34,40] i.e.,

$$f_N = \sum_{i=1}^{p} f_i \,\{1 - \exp[-k_i\,(f_c)^{n_i}\,] \qquad \text{(SI-2.5.)}$$

For the sub-systems S1-1, S2-1, S1-4, S2-4., S1-7 and S2-7., the parameters f_i, k_i and n_i were determined by fitting of the measured relationships between f_N and f_c (symbols ○, ▲ and ▽ in Fig. 5 of the paper) and listed in Table SI-2.1.

Table SI-2.1. Numerical values of the constants f_i, k_i and n_i in Eqs. (SI-2.5) and (SI-2.9), used in simulation.

Sub-system	S1-1	S2-1	S1-4	S2-4	S1-7	S2-7
f_1	1.35E-3	1.0E-3	2.4E-3	4.25E-4	9.0E-4	1.05E-4
k_1	130.32	78.257	135.639	1.823E3	92.7586	417.799
n_1	0.51	0.48	0.39	0.3917	0.385	0.415
f_2	2.4E-3	1.6E-3	4.0E-3	1.6E-3	1.7E-3	5.5E-4
k_2	1.4952E3	4.8659E3	2.7173E4	1.4723E5	2.515E3	6.108E4
n_2	1.09	1.31	1.045	0.96	0.94	1.02
f_3	9.0E-3	5.0E-3	0.01	1.9E-3	0.01	4.75E-4
k_3	27.66	2.3861E4	9.295E6	2.4639E9	2.465E3	3.991E10
n_3	1.08	2.08	1.99	2.03	1.44	2.66
f_4	7.0E-3	7.0E-3	0.016	5.5E-3	0.024	5.0E-4
k_4	114.434	8.8205E5	6.125E11	1.242E9	2.159E4	4.886E13
n_4	2.69	3.7	3.82	2.28	2.48	3.9
f_5	2.6E-3	0.012	0.045	0.045	0.1	1.8E-3
k_5	21.758	6.6342E3	1.4045E7	3.516E3	5.324E3	2.566E6
n_5	3.55	3.22	2.75	1.28	3.05	2.22
f_6	0.3	0.0107	0.05	0.08	0.2	0.016
k_6	32.9503	2.1E3	2.89124E12	2.0898EE5	3.1257E4	1.054E3
n_6	23.9	3.9	5.72	2.45	5.04	1.62
f_7	0.67765	0.6	0.12	0.2	0.2	0.12
k_7	109.974	103.5444	5.498E7	1.954E4	3.181E5	518.013
n_7	46.4	13.0	4.35	2.62	8.1	2.48
f_8		0.3627	0.25	0.19075	0.34	0.2
k_8		9.676E4	7.8433E4	93.691	2.276E3	1.794E3
n_8		45.4	3.7	3.02	6.65	4.34
f_9			0.0826	0.124825	0.1234	0.22057
k_9			78.571	1.083E4	3.2365E6	1.0378E5
n_9			3.74	4.8	16.8	14
f_{10}			0.42	0.35		0.44
k_{10}			252.144	1.339E3		943.881
n_{10}			2.69	2.7		5.85

The curves in Fig. 5 of the paper are calculated by Eq. (SI-2.5.) using the appropriate values of the constants f_i, k_i and n_i, listed in Table SI-2.1.

The first derivative of Eq. (SI-2.5) gives,

$$\mathrm{d}f_N/\mathrm{d}f_c = \sum_{i=1}^{p} f_i\, k_i\, n_i\, (f_c)^{(n_i-1)} \exp[-k_i\, (f_c)^{n_i} \tag{SI-2.6}$$

and thus, in accordance with Eq. (4) of the paper, the density function, $F(\mathrm{N})$, of distribution of nuclei in the gel matrix, is,

$$F(\mathrm{N}) = N_s(\mathrm{d}f_N/\mathrm{d}f_c) = N_s \times \sum_{i=1}^{p} f_i\, k_i\, n_i\, (f_c)^{(n_i-1)} \exp[-k_i\, (f_c)^{n_i} \tag{SI-2.7}$$

where, N_s is the specific number of nuclei (number of nuclei "released" from a unit mass of dissolved gel). Since the general form of the kinetics of autocatalytic nucleation is,[7,34,39,40]

$$B = \mathrm{d}N/\mathrm{d}t_c = F(\mathrm{N})(\mathrm{d}m_c/\mathrm{d}t_c) \tag{SI-2.8}$$

the kinetics of autocatalytic nucleation, for given distribution of nuclei in the gel matrix, can be obtained by combination of Eqs. (SI-2.7) and (SI-2.8) in the form

$$\mathrm{d}N/\mathrm{d}t_c = N_s\{\sum_{i=1}^{p} f_i\, k_i\, n_i\, (f_c)^{(n_i-1)} \exp[-k_i\, (f_c)^{n_i}]\}(\mathrm{d}f_c/\mathrm{d}t_c) \tag{SI-2.9}$$

Analyzes of many kinetics of crystal growth of zeolites resulted in a finding that the typical profile of zeolite growth rate curves (see Figs. 3Ad, 3Bd, 4Ad and 4Bd in the paper) may be perfectly simulated by a solution of the differential equation,[3,4,7,40]

$$Q = \mathrm{d}D/\mathrm{d}t_c = K_g \times \{1 - \exp[K_d \times (D - D_{max})]\} \tag{SI-2.10}$$

where, K_g is the rate constant of linear crystal growth, D_{max} is the size (equivalent spherical diameter; see SI-I) of the largest crystals at the end of the crystallization process, i.e., $D_{max} = D_m(\mathrm{end})$ (plateau of the D vs. t_c curves (see Figs. 3Ad, 3Bd, 4Ad and 4Bd in the paper) and K_d is the factor which determines the deviation of D vs. t_c function from linearity.[3,7,39-41] A combination of Eqs. (SI-2.2) – (SI-2.4) and (SI-2.10) gives,

$$\mathrm{d}m_1/\mathrm{d}t_c = K_g \times \{1 - \exp[K_d \times (D - D_{max})]\} \times m_o \tag{SI-2.11}$$

$$\mathrm{d}m_2/\mathrm{d}t_c = 2 \times K_g \times \{1 - \exp[K_d \times (D - D_{max})]\} \times m_1 \tag{SI-2.12}$$

$$\mathrm{d}m_3/\mathrm{d}t_c = 3 \times K_g \times \{1 - \exp[K_d \times (D - D_{max})]\} \times m_2 \tag{SI-2.13}$$

Thus, the changes in f_c, D and $\mathrm{d}N/\mathrm{d}t_c$ during crystallization can be calculated (simulated) by simultaneous solution of differential Eqs. (SI-2.9), (SI-2.11), (SI-2.12) and (SI-2.13), using the corresponding values of the constants N_s, K_g, D_{max} (see Table 3 in the paper) and the initial values of $m_i(t_c = 0) = N(t_c = 0) \times [D(t_c = 0)]^i$ and $D(t_c = 0)$. Since $m_G^* = 0$ at $t_c = 0$, no nuclei are released at $t_c = 0$, and thus $m_o(0) = N(t_c = 0) = 0$. However, since in many cases the condition, $m_o(0) > 0$ must be satisfied to start the simulation, $m_o(0) = 100\#$ is appropriate value; this is enough for the start of calculation/simulation and at the same time too small to influence the result of calculation/simulation in any case. Consequently, for usually used size of nuclei, i.e., $D(t_c = 0) =$

10^{-7} cm,[3,6,7,37,38,40,68] $m_1(t_c = 0) = N(t_c = 0)\times D(t_c = 0) = 10^{-5}$ # cm, $m_2(t_c = 0) = N(t_c = 0)\times[D(t_c = 0)]^2 = 10^{-12}$ # cm^2 and $m_3(t_c = 0) = N(t_c = 0)\times[D(t_c = 0)]^3 = 10^{-19}$ # cm^3 for all analyzed systems in the paper.

The mass fraction, f_c, of crystallized zeolite A was calculated as,[3,6,7,39,40,69]

$$f_c = G\times\rho\times m_3 \qquad \text{(SI-2.14)}$$

where $G = \pi/6$ and $\rho = 2$ g/dm^3 are the geometrical shape factor (spheres) and density of growing zeolite crystals. Crystal size distributions by number, dN/dD of the crystalline end products were calculated by the solution of the general form of population balance equation,[68,70] i.e.,

$$\mathrm{d}N/\mathrm{d}D = -(1/Q)\times \mathrm{d}N/\mathrm{d}t_c = -(\mathrm{d}N/\mathrm{d}t_c)/Q = -(\mathrm{d}N/\mathrm{d}t_c)/K_g\{1 - \exp[K_d\times(D - D_{max})]\} \qquad \text{(SI-2.15)}$$

Consequently, crystal size distribution by volume (mass), dV/dD, was calculated as,

$$\mathrm{d}V/\mathrm{d}D = -[(\mathrm{d}N/\mathrm{d}t_c)\times(\int_{D(t_c=0)}^{D} Q\mathrm{d}t_c)^3]/Q \qquad \text{(SI-2.16)}$$

Additional reference

70 A. D. Randolph, M. A. Larson, *Theory of Particulate Processes*, Academic Press, New York, NY, 1971, pp. 12–63.

SI-3: The relationship between the alkalinity, A, and the growth rate constant, K_g

Previous investigations of the kinetics of crystal growth of zeolite A[3,56,57] showed that the rate, R_g, of crystal growth can be expressed as,

$$R_g = \mathrm{d}D/\mathrm{d}t_c = r_g \times F(C) = r_g \times C_{Na} \times (C_{Al} - C_{Al}^*) \times (C_{Si} - C_{Si}^*) \qquad \text{(SI-3.1)}$$

where, D is the crystal size at the crystallization time t_c, r_g is the crystal growth rate constant, C_{Na}, C_{Al} and C_{Si} are the concentrations of sodium, aluminum and silicon in the liquid phase during crystallization and C_{Al}^* and C_{Si}^* are the concentrations of aluminium and silicon in the liquid phase which correspond to the solubility of zeolite A at given crystallization conditions.

In most of zeolite crystallization, crystal size, D, increases linearly during the main part of the crystallization process,[3,7,8,12,35,36,40,49] and thus,

$$R_g = \mathrm{d}D/\mathrm{d}t_c = K_g \qquad \text{(SI-3.2)}$$

Analizes of many kinetics of zeolite crystal growth have shown that for given composition of the reaction mixture, the constancy of R_g during the main part of the crystallization is the consequence of the constancy of the concentration factor $F(C) = F(C)_{const}$ in the same time interval[3,56,57,71] and thus,

$$K_g = r_g \times F(C)_{const} \qquad \text{(SI-3.3)}$$

The same analyzes have shown that the value of r_g non-lineary decreases and the value of $F(C)_{const}$ non-lineary increases with increasing alkalinty; the increase of $F(C)_{const}$ is caused by the increase of both the concentration differences $(C_{Al} - C_{Al}^*)$ and $(C_{Si} - C_{Si}^*)$ with increasing alkalinity[56]**.** An investigation of the influence of concentration of Na^+ ions on the kinetics of crystal growth of zeolite A showed that, at constant alkalinity, the value of K_g linearly increases with the concentration of sodium sulfate (concentration of Na^+ ions) added into the reaction mixture.[57] Finally, an investigation of the influence of different anions on the kinetics of crystal growth of zeolite A showed, that only sodium ions and not associated anions influence the rate of crystal growth of zeolite A.[72]

From these finding is evident that simultaneous increase of Na^+ and OH^- ions (increase of alkalinity, A) increases the value of $F(C)_{const}$ by simultaneous increase of C_{Na}, $(C_{Al} - C_{Al}^*)$ and $(C_{Si} - C_{Si}^*)$ and, at the sime time, decreases the value of r_g. Since the decrease of r_g is slower than the increase of $F(C)_{const}$,[56] the value of K_g increases with increasing alkalinity of the reaction mixture[3,56,63,73] (see also the data in Table 3 of the paper).

The combined influence of the alkalinity, A, on r_g and $F(C)_{const}$ is a possible reason that K_g is not a linear, but, as expected on the basis of previous analyzes,[3,63,72] a power function of A, i.e,

$$K_g = K \times A^r \qquad \text{(SI-3.4)}$$

where the values $K = 9.43\times10^{-3}$ and $r = 1.204$ for system S1 and $K = 3.062\times10^{-3}$ and $r = 1.27$ for system S2 were calculated as the intersections with y-axes and slopes of the corresponding log K_g vs. log A functions (see Fig. SI-3.1).

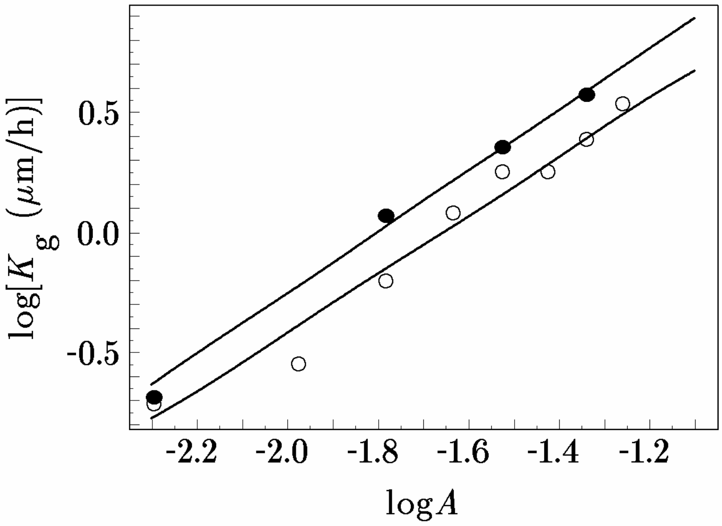

Fig. SI-3.1. Logarithmic presentation of the relationship between alkalinity, *A*, and the values of K_g which correspond to the systems S1 (○) and S2 (●).

Additional References

71 S. Bosnar, B. Subotić, *Croat. Chem. Acta* 2002, **75**, 663.

72 S. Bosnar, T. Antonić Jelić, J. Bronić, I. Krznarić, B. Subotić, *J. Cryst. Growth* 2004, **267**, 270.

73 A. Iwasaki, I. Kudo, T. Sano, *Stud. Surf. Sci. Catal.* 1997, **105**, 317

SI-4. Analysis of the crystallization processes under different conditions

Because of close (systems S1-4 and S2-4; Fig. SI-4.1D) or even the same (systems S1-1 and S2-1.; Fig. 8D in the paper) rates of crystal growth, it is evident that a considerable differences in the kinetics of crystallization from hydrogels having the same alkalinity, but different ratio $[SiO_2/Al_2O_3]_b$, is determined by the kinetics of nucleation and thus, by both specific number of nuclei, N_s, and distribution of nuclei in the gel matrix. Since, on the other hand, the distributions of nuclei in the systems S1-4 and S2-4 are the same (see Fig. 6B in the paper), the higher rate of nucleation in system S2-4 (maximum rate of nucleation, $(dN/dt_c)_{max} = 8.65\times10^{10}$ # g^{-1} h^{-1} is reached at $t_c = 2.65$ h; see Table 3) than in system S1-4 (maximum rate of nucleation, $(dN/dt_c)_{max} = 4.83\times10^{10}$ # g^{-1} h^{-1} is reached at $t_c = 3.6$ h; see Table 3) is obviously the consequence of higher specific number of nuclei in system S2-4. ($N_s = 8.66\times10^{10}$ # g^{-1}; see Table 3) than in system S1-4 ($N_s = 6.72\times10^{10}$ # g^{-1}; see Table 3). On the other hand, although the distributions of nuclei in the systems S1-7 and S2-7 are almost the same (see Fig. 6D in the paper) and both N_s (= 4.22×10^{11} # g^{-1}) and $(dN/dt_c)_{max}$ (=1.491×10^{12} # g^{-1} h^{-1}) in system S1-7 are slightly higher than N_s (= 3.22×10^{11} # g^{-1}) and $(dN/dt_c)_{max}$ (=1.362×10^{12} # g^{-1} h^{-1}) in system S2-7., the overall rate of crystallization is higher in system S2-7 than in system S1-7. (see Fig. SI-4.2A). Obviously, the reason is considerably higher rate of crystal growth in system S2-7 than in system S1-7 (see Fig. SI-4.2D).

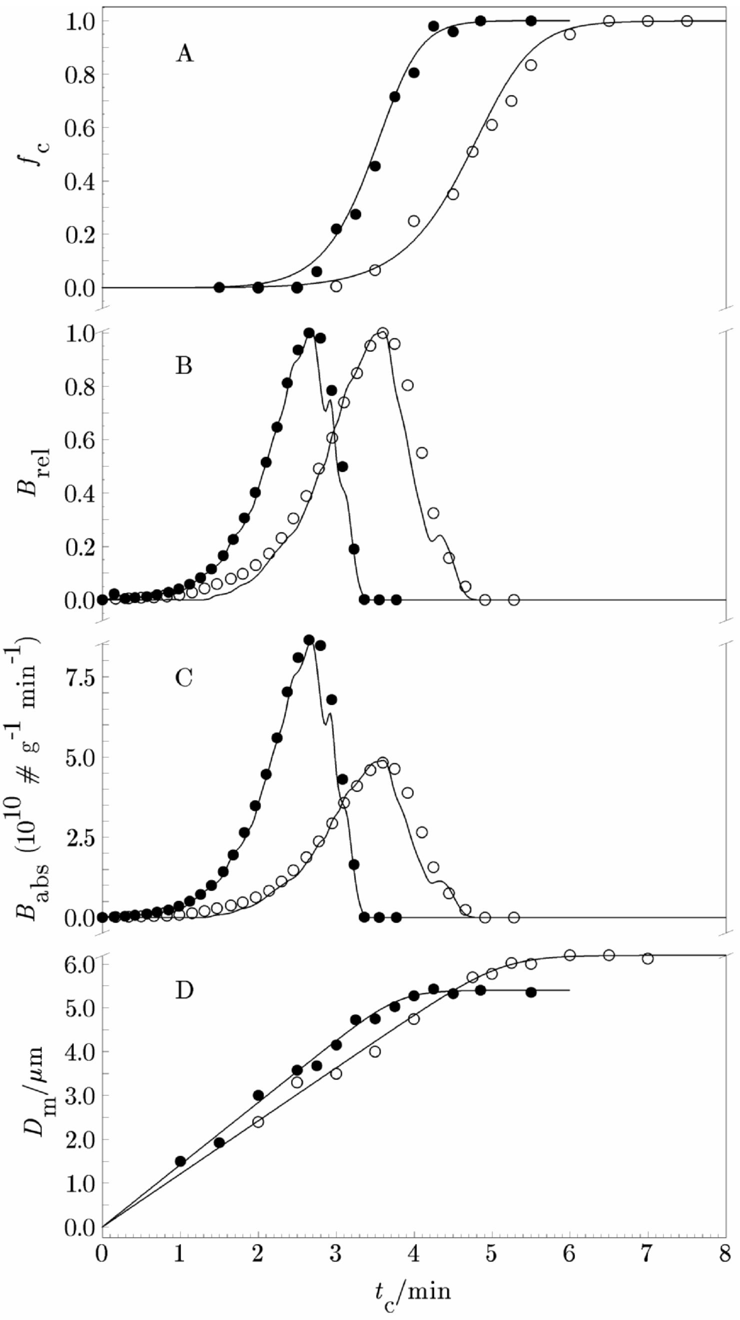

Fig. SI-4.1 Measured (points) and calculated (simulated; curves) changes of: (A) fractions, f_c, of crystallized zeolite A, (B) relative rates, B_{rel} , of nucleation, (C) absolute rates, B_{abs}, of nucleation and (D) size (equivalent spherical diameter, D_m) of the largest zeolite A crystals during crystallization of zeolite A in sub-systems S1-4 (○) and S2-4 (●). t_c is the time of crystallization.

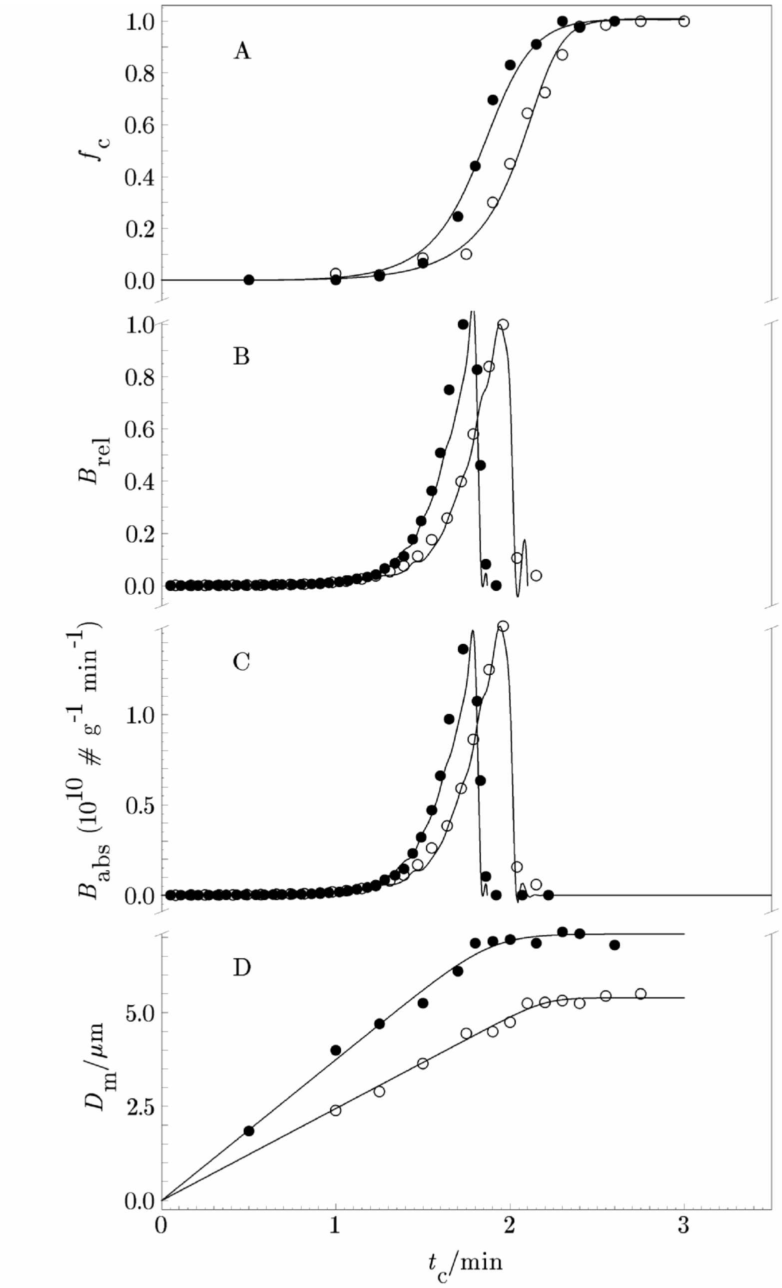

Fig. SI-4.2 Measured (points) and calculated (simulated; curves) changes of: (A) fractions, f_c, of crystallized zeolite A, (B) relative rates, B_{rel} , of nucleation, (C) absolute rates, B_{abs}, of nucleation and (D) size (equivalent spherical diameter, D_m) of the largest zeolite A crystals during crystallization of zeolite A in sub-systems S1-7 (○) and S2-7. (●). t_c is the time of crystallization.